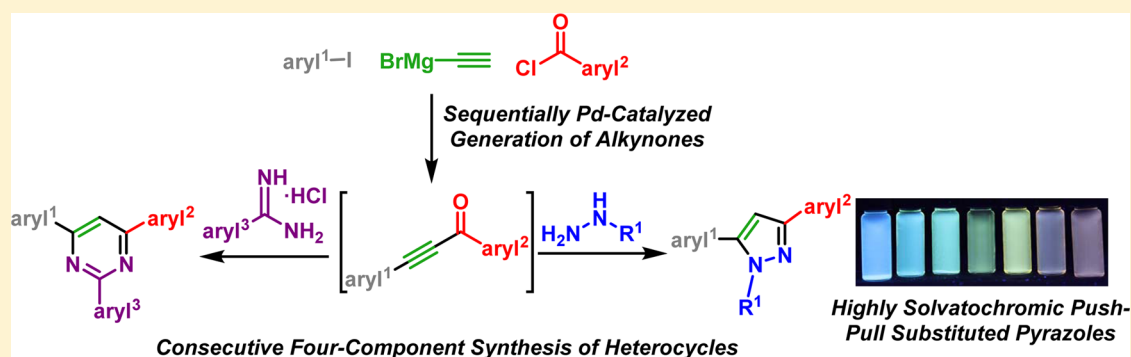


One-Pot Coupling–Coupling–Cyclocondensation Synthesis of Fluorescent Pyrazoles

Alissa C. Götzinger, Florian A. Theßeling, Corinna Hoppe, and Thomas J. J. Müller^{*,†}

Institut für Organische Chemie und Makromolekulare Chemie, Heinrich-Heine-Universität Düsseldorf, Universitätsstraße 1, D-40225 Düsseldorf, Germany

S Supporting Information



ABSTRACT: Consecutive four-component coupling–coupling–cyclocondensation syntheses of pyrazoles and pyrimidines were developed by taking advantage of the provisional, sequentially Pd-catalyzed one-pot generation of alkynones from aryl iodides, ethynylmagnesium bromide, and acid chlorides. This one-pot methodology allows the concise, diversity-oriented generation of a set of donor-, acceptor-, and donor–acceptor-substituted pyrazoles, which are interesting fluorophores. Most distinctly, donor–acceptor pyrazoles display remarkably red-shifted emission maxima and pronounced positive solvochromicity, spanning an overall range from 363 nm (cyclohexane) to 595 nm (acetonitrile). DFT and TD-DFT calculations elucidate the electronic structure and the photophysical behavior. Upon photonic excitation, considerable charge-transfer character becomes apparent, which rationalizes the origin of huge Stokes shifts and solvochromic behavior.

INTRODUCTION

Pyrazoles possess interesting photophysical properties as UV absorbers¹ and have received considerable attention in technological applications, e.g., as optical brighteners in detergents,² UV stabilizers for polystyrene,³ and highly selective fluorescence sensors.⁴ Furthermore, pyrazoles often display blue emission and large Stokes shifts, which makes them particularly interesting for OLED technologies.⁵ In addition, applications of pyrazoles in dye-sensitized solar cells⁶ and in nonlinear optics^{1a,b} have been considered. Therefore, novel syntheses of pyrazoles remain highly attractive evergreens in heterocyclic chemistry.

Challenged by the photophysical profile of pyrazoles as fluorophores and the ongoing mission to access tailor-made π -systems by diversity-oriented syntheses (DOS)⁷ such as multicomponent reactions (MCR),⁸ we have developed regioselective consecutive three- and four-component Sonogashira coupling–cyclocondensation(–coupling) syntheses of fluorescent 1,3,5-trisubstituted and 1,3,4,5-tetrasubstituted pyrazoles in a one-pot fashion.⁹ In this context, we could probe and efficiently illustrate the concept of sequentially Pd-catalyzed processes¹⁰ for one-pot syntheses of pyrazoles^{9a} by concatenating Sonogashira and Suzuki coupling in a one-pot fashion intercepted by cyclocondensation.

Alkynones are particularly useful electrophilic three-carbon building blocks in the synthesis of heterocyclic compounds.¹¹ We have very recently reported a sequentially palladium-catalyzed synthesis of alkynones **4** from aryl iodides **1** by in situ generation of terminal alkynes via a Kumada-type coupling with ethynylmagnesium bromide (**2**)¹² followed by a Sonogashira coupling with aryl chlorides **3** (Scheme 1).¹³

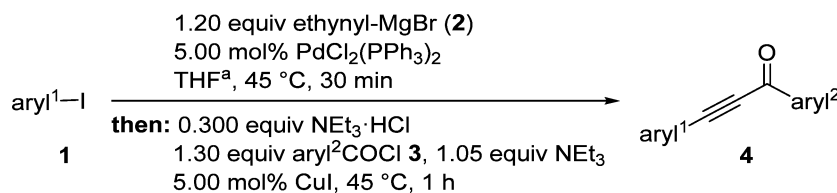
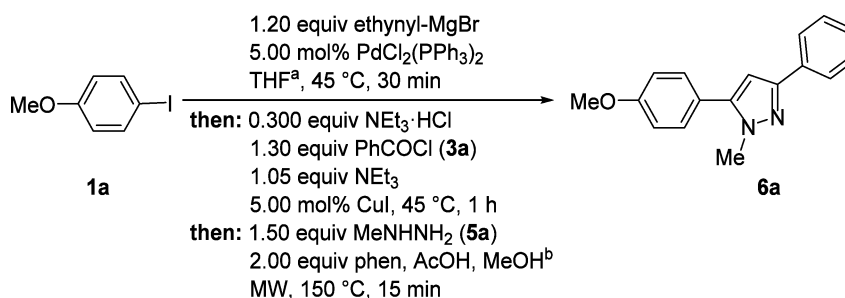
The modular, diversity-oriented, and catalyst-economical nature of this sequence allows for quick and convenient synthesis of diversely substituted examples, combining short reaction times, easy workup, and readily available starting materials.

Here, we report the concatenation of this sequentially Pd-catalyzed alkynone formation with cyclocondensation, giving direct access to functional heterocycles in the sense of a consecutive four-component coupling–coupling–cyclocondensation process. In addition, photophysical properties and studies on the electronic structure of selected novel 1,3,5-trisubstituted pyrazoles are reported and discussed.

Special Issue: Heterocycles

Received: June 1, 2016

Published: July 12, 2016

Scheme 1. Sequentially Pd-Catalyzed Three-Component Kumada–Sonogashira Synthesis of Alkynones 4^{a, 13}^ac₀(1a) = 0.42 M.Scheme 2. Optimized Conditions for the Four-Component Synthesis of Pyrazole 6a^{a, b}^ac₀(1a) = 0.42 M. ^bV(MeOH) = V(AcOH) = 0.4 mL/mmol.

RESULTS AND DISCUSSION

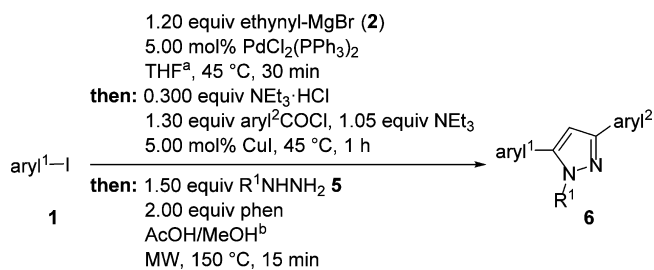
Synthesis. We first set out to investigate the consecutive four-component synthesis of pyrazoles **6**. As shown in previous coupling–cyclocondensation studies, the cyclocondensation step can be considerably accelerated using microwave irradiation in the presence of acetic acid and methanol as a polar cosolvent.^{9,14} Extensive optimization studies, particularly on the conditions of the terminal cyclocondensation, were conducted employing 4-iodoanisole (**1a**), ethynylmagnesium bromide (**2**), benzoyl chloride (**3a**), and methyl hydrazine (**5a**) to give 5-(4-methoxyphenyl)-1-methyl-3-phenyl-1H-pyrazole (**6a**) as a model reaction (Scheme 2). Most importantly, the presence of magnesium ions considerably hampered the cyclocondensation with methyl hydrazine (**3a**), presumably due to competing coordination. This problem was solved by employing a slight excess of hydrazine **3a** and by addition of phenanthroline as a coordinating ligand for Mg²⁺. Consequently, model pyrazole **6a** could be isolated in 77% yield.

With these modified conditions in hand, the consecutive four-component coupling–coupling–cyclocondensation synthesis of 3,5-diarylpyrazoles **6** was illustrated in 17 preparative examples, furnishing the title compounds in moderate to very good yields (Table 1).

In most cases, the synthesis is completely regioselective; only for a few derivatives is the corresponding regioisomer placing aryl **1** in position **3** obtained as a side product (Table 1, entries 1 and 7). The modular nature of the reaction allows introduction of a variety of aryl substituents bearing electron-donating as well as electron-withdrawing substituents. When phenyl hydrazine is used, a 1:2 mixture of regioisomers is obtained. As previously shown for aryl hydrazines, the Michael attack of the terminal hydrazine nitrogen atom becomes prevalent due to the reduced electron density at the internal nitrogen atom, contrary to the behavior of aliphatic hydrazines.^{9b}

When 1,4-diiodobenzene (**1b**) is employed as an aryl iodide, 1,4-bis(1-methyl-3-phenyl-1H-pyrazol-5-yl)benzene (**6r**) can be obtained in 57% yield (Scheme 3). Taking into account

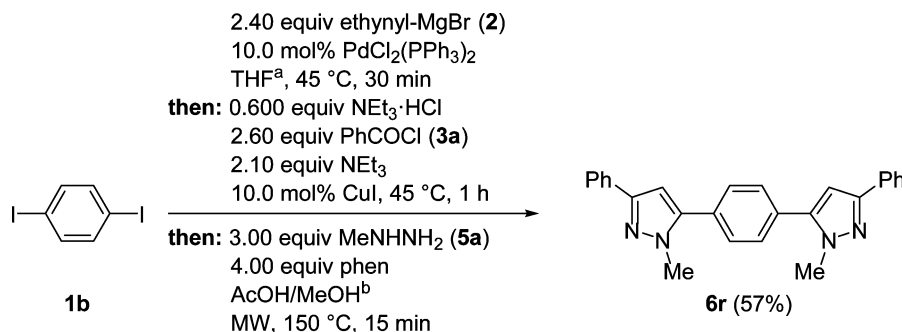
Table 1. Consecutive Four-Component Coupling–Coupling–Cyclocondensation Synthesis of Pyrazoles **6** from Aryl Iodides **1**, Ethynylmagnesium Bromide (**2**), Aryl Chlorides **3**, and Hydrazines **5**^{a, b}



entry	aryl ¹	aryl ²	R ¹	pyrazole 6 (yield, %) ^c
1	4-MeOC ₆ H ₄	Ph	Me	6a ^d (77)
2	4-MeOC ₆ H ₄	Ph	H	6b (68)
3	4-ClC ₆ H ₄	Ph	Me	6c (68)
4	4-ClC ₆ H ₄	4-Tol	Me	6d (59)
5	4-ClC ₆ H ₄	Ph	H	6e (64)
6	Ph	4-Tol	Me	6f (79)
7	2-naphthyl	Ph	Me	6g ^d (70)
8	OCF ₃	Ph	Me	6h (58)
9	Ph	Ph	Me	6i (72)
10	Ph	4-F ₃ CC ₆ H ₄	Me	6j (44)
11	Ph	4-NCC ₆ H ₄	Me	6k (35)
12	4-MeOC ₆ H ₄	4-F ₃ CC ₆ H ₄	Me	6l (58)
13	4-MeOC ₆ H ₄	4-NCC ₆ H ₄	Me	6m (43)
14	Me ₂ NC ₆ H ₄	Ph	Me	6n (60)
15	Me ₂ NC ₆ H ₄	4-F ₃ CC ₆ H ₄	Me	6o (58)
16	Me ₂ NC ₆ H ₄	4-NCC ₆ H ₄	Me	6p (60)
17	4-MeOC ₆ H ₄	Ph	Ph	6q ^c (47)

^ac₀(1a) = 0.42 M. ^bV(MeOH) = V(AcOH) = 0.4 mL/mmol.^cIsolated yield (after chromatography on silica gel). ^dRegioisomeric ratio of 10:1 (determined by 1H NMR). ^eRegioisomeric ratio of 1:2 (determined by 1H NMR).

Scheme 3. Pseudo-Seven-Component Coupling–Coupling–Cyclocondensation Synthesis of 1,4-Bis(1-methyl-3-phenyl-1H-pyrazol-5-yl)benzene (6r) from 1,4-Diiodobenzene (1a), Ethynylmagnesium Bromide (2), Benzoyl Chloride (3a), and Methylhydrazine (5a)^{a,b}

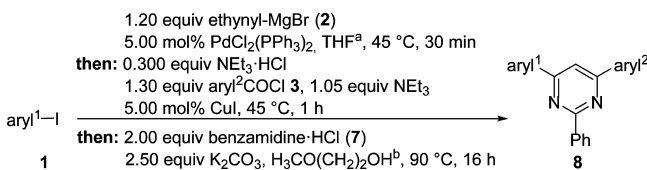


^a $c_0(1a) = 0.21$ M. ^b $V(\text{MeOH}) = V(\text{AcOH}) = 0.8$ mL/mmol. phen: phenanthroline (ligand).

that eight bonds are formed in a pseudo-seven-component fashion, the average yield per bond-forming step accounts to 93%.

We could also establish a consecutive four-component coupling–coupling–cyclocondensation synthesis of 2,4,6-tri-aryl-substituted pyrimidine derivatives by employing benzamidine chloride (7) as a precursor of the bifunctional nucleophile (Table 2).¹⁵

Table 2. Consecutive Four-Component Coupling–Coupling–Cyclocondensation Synthesis of Pyrimidines 8 from Aryl Iodides 1, Ethynylmagnesium Bromide (2), Aryl Chlorides 3, and Benzamidine Hydrochloride (7)^{a,b}



product	aryl ¹	aryl ²	yield ^c (%)
8a	4-MeOC ₆ H ₄	Ph	51
8b	4-Tol	Ph	43
8c	2-naphthyl	4-Tol	46
8d	4-F ₃ CC ₆ H ₄	Ph	42
8e	4-ClC ₆ H ₄	Ph	43
8f	4-BrC ₆ H ₄	3-ClC ₆ H ₄	49

^a $c_0(1a) = 0.42$ M. ^b $V(\text{H}_3\text{C}(\text{CH}_2)_2\text{OH}) = 2.0$ mL/mmol. ^cAfter chromatography on silica gel and recrystallization, if necessary.

The use of microwave irradiation did not prove to be beneficial; neither did the addition of phenanthroline as a ligand for Mg²⁺. Conventional heating for 16 h at 90 °C (oil bath) with 2 equiv of benzamidine hydrochloride (7) in the presence of potassium carbonate and 2-methoxyethanol as a polar cosolvent turned out to be most favorable. Under these conditions, six pyrimidine derivatives 8 were obtained in moderate yields.

Photophysical Properties of Push–Pull Substituted Pyrazoles. Previous studies on 3,5-diarylpyrazoles have shown interesting photophysical properties,^{9a} especially for donor–acceptor-substituted diarylmethylpyrazoles, which display bathochromically shifted emission maxima and large Stokes shifts.^{9b} Because of the polar auxochrome and anti-auxochrome substituents, solvochromic emission properties can also be expected.

For a more systematic treatment of this phenomenon, various combinations of donor and acceptor substituents were considered. While 4-methoxy- and 4-(dimethylamino)phenyl were introduced as donors at position 5 by aryl iodide 1, 4-cyanobenzoyl chloride and 4-(trifluoromethyl)benzoyl chloride enabled access to the corresponding 3-acceptor-substituted pyrazoles. In each case, the synthesized corresponding donor (6a,n), acceptor (6j,k), and donor–acceptor-substituted (6l,m,o,p) pyrazole derivatives were characterized by absorption and emission spectroscopy (Table 3).

Table 3. Selected UV/Vis Absorption and Emission Data of Pyrazoles 6a,i–p

structure	$\lambda_{\text{max,Abs}}^a$ (nm) (ϵ (M ⁻¹ cm ⁻¹))	$\lambda_{\text{max,Em}}^{b,c}$ (nm) (Φ_F)	$\Delta\tilde{\nu}$ (cm ⁻¹)
6a	257 (37640)	333 (0.21)	8900
6i	254 (33534)	338 (0.42)	9800
6j	260 (20709)	341 (0.52)	9100
6k	282 (27398)	348 (0.70)	6700
6l	262 (34792)	367 (0.20)	10900
6m	281 (35307)	394 (0.30)	10300
6n	280 (29184)	365 (0.06)	8300
6o	283 (31218)	448 (0.11)	13000
6p	292 (40062)	499 (0.21)	14100

^aRecorded in dichloromethane, $T = 293$ K, $c(6) = 10^{-5}$ M. ^bRecorded in dichloromethane, $T = 293$ K, $c(6) = 10^{-7}$ M. ^cFluorescence quantum yields were determined relative to diphenyloxazole ($\Phi_F = 0.84$)¹⁶ as a standard in cyclohexane.

The absorption maximum of the parent compound, diphenyl derivative 6i, lies at 254 nm. Generally, separate donor as well as separate acceptor substitution leads to a modest bathochromic shift of the longest wavelength absorption band. The absorption maxima of methoxy- and trifluoromethyl-substituted derivatives 6a and 6j can be found at 257 and 260 nm, respectively, while 6k and 6n, carrying a cyano and a dimethylamino group, exhibit absorption maxima at 282 and 280 nm. However, the absorption maximum of push–pull-substituted derivative 6p bearing both a dimethylamino and a cyano moiety is most bathochromically shifted. Figure 1 shows the absorption and emission spectra of donor–acceptor substituted pyrazoles 6l,m,o,p.

The emission maximum of parent diphenyl derivative 6i lies at 338 nm with a Stokes shift of 9800 cm⁻¹. Introduction of the weaker methoxy donor (6a) or trifluoromethyl acceptor (6j)

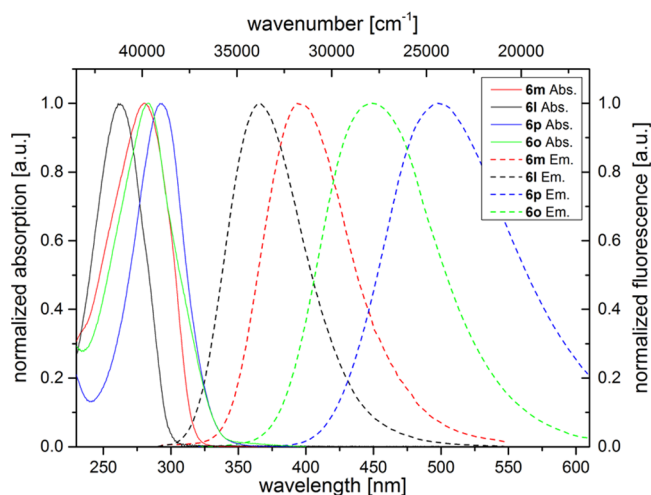


Figure 1. UV/vis absorption (solid lines) and emission (dashed lines) spectra of donor–acceptor-substituted pyrazoles **6l,m,o,p**. Recorded in dichloromethane, $T = 293$ K.

only moderately affects the emission energy, while introduction of the strong dimethylamino donor (**6n**) leads to a substantial bathochromic shift to 365 nm. Acceptor-substituted pyrazole **6k** bearing the stronger cyano moiety also shows a red-shifted emission maximum at 348 nm. In these cases, smaller Stokes shifts can be found since the shift in absorption is more pronounced than that in emission. Methoxy-substituted derivatives **6l** and **6m** with a trifluoromethyl or cyano acceptor functionality exhibit a stronger bathochromic shift to 367 and 394 nm, respectively, while push–pull systems **6o** and **6p** carrying a dimethylamino donor functionality create the strongest red shifts with emission maxima at 448 and 499 nm. In these cases, extraordinarily large Stokes shifts of 13000 and 14100 cm^{-1} can be determined. The decadic molar extinction coefficients of the absorption bands lie between 20000 and 40000 $\text{M}^{-1} \text{cm}^{-1}$, with the strongest absorption for push–pull derivative **6p**. Dimethylamino-substituted compound **6n** is the only one to exhibit a second, longer wavelength emission maximum at 489 nm, which probably stems from a twisted intramolecular charge transfer.¹⁷ Relative fluorescence quantum yields¹⁸ were measured with diphenyloxazole as a standard in cyclohexane ($\Phi_F = 0.84$),¹⁶ and a variation with donor and acceptor strength is observed. Introduction of donor substituents appears to have a detrimental effect on quantum yield, with only 6% for dimethylamino-substituted derivative **6n**. Acceptor substitution, however, appears to increase fluorescence efficiency, so that the

highest relative quantum yield of 70% can be found for cyano-substituted derivative **6k**.

Intrigued by the strongly red-shifted emission, we undertook solvochromicity studies with dimethylamino–cyano-substituted pyrazole **6p** to scrutinize the effect of the solvent environment on its absorption and emission properties. It is visually evident that compound **6p** exhibits a positive emission solvatochromism; i.e., the emission is shifted bathochromically with increasing solvent polarity (Figure 2).

This effect was further investigated by recording absorption and emission spectra in solvents with different solvent polarities (Figure 3). Interestingly, the absorption maximum exhibits no

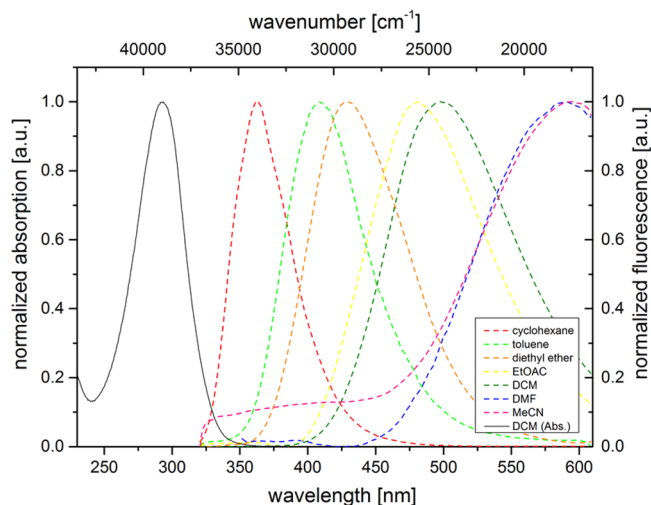


Figure 3. UV/vis absorption in dichloromethane (solid line) and emission (dashed lines) spectra in seven solvents of different polarity (recorded at $T = 293$ K).

solvatochromicity, with the maximum remaining almost unchanged at between 298 and 295 nm. On the other hand, the influence of the solvent polarity on the emission maximum is very pronounced, with maxima ranging from 362 nm in cyclohexane to 595 nm in acetonitrile (Table 4). This positive solvatochromism correlates with a considerable increase of the dipole moment upon photonic excitation.¹⁹

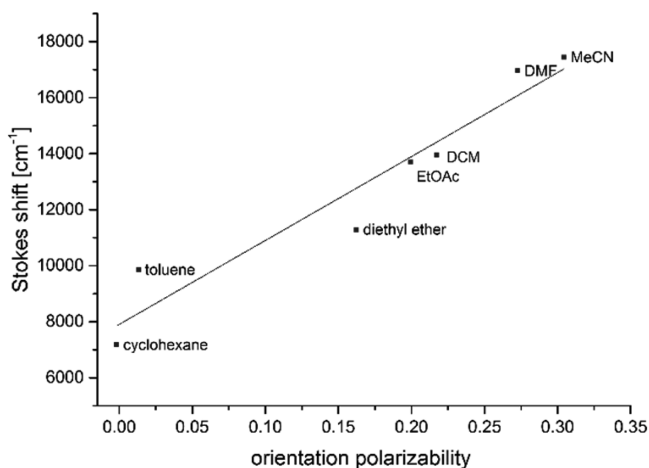
Plotting the Stokes shifts $\Delta\bar{\nu}$ against the orientation polarizabilities Δf of the respective solvent (Lippert plot) furnished a good linear correlation with a fit of $r^2 = 0.92$ (Figure 4). Orientation polarizabilities Δf (eq 1) were calculated according to



Figure 2. Fluorescence of **6p** with variable solvent polarity (left to right: cyclohexane, toluene, ethyl acetate, dichloromethane, *N,N*-dimethylformamide, acetonitrile; $\lambda_{\text{exc}} = 365$ nm, hand-held UV lamp).

Table 4. UV/vis Absorption and Emission Data for **6p** in Seven Solvents of Different Polarity

solvent	$\lambda_{\max, \text{Abs}}$ (nm)	$\lambda_{\max, \text{Em}}$ (nm)	$\Delta\tilde{\nu}$ (cm^{-1})
cyclohexane	288	363	7200
toluene	292	410	9900
diethyl ether	289	429	11300
ethyl acetate	290	481	13700
dichloromethane	294	498	13900
<i>N,N</i> -dimethylformamide	295	590	16900
acetonitrile	292	595	17400

**Figure 4.** Lippert plot for compound **6p** ($n = 7$, $r^2 = 0.92$).

$$\Delta f = \frac{\epsilon_r - 1}{2\epsilon_r + 1} - \frac{n^2 - 1}{2n^2 + 1} \quad (1)$$

from the relative permittivity ϵ_r and the optical refractive index n of the respective solvent.

The change in dipole moment from the ground to the excited state can be calculated using SI units in the Lippert–Mataga equation (eq 2)²⁰

$$\tilde{\nu}_a - \tilde{\nu}_f = \frac{2\Delta f}{4\pi\epsilon_0 h c a^3} (\mu_E - \mu_G)^2 + \text{const} \quad (2)$$

where $\Delta\tilde{\nu}_a$ and $\Delta\tilde{\nu}_f$ represent the absorption and emission maxima (in m^{-1}), μ_E and μ_G are the dipole moments in the excited and ground state (in Cm), ϵ_0 (8.8542×10^{-12} As V^{-1} m^{-1}) is the vacuum permittivity constant, h (6.6256×10^{-34} J s) is Planck's constant, c (2.9979×10^8 m s^{-1}) is the speed of light, and a is the radius of the solvent cavity occupied by the molecule (in m).

The Onsager radius a , which is used to approximate the molecular volume of the molecule in solution, was estimated from the optimized ground-state structure obtained by DFT calculations. Using a value of 8.7 Å (8.7×10^{-10} m), the change in dipole moment was calculated to be $\Delta\mu = 46$ D (1.54×10^{-28} Cm). This remarkably large value corresponds to a pronounced charge separation.

Calculated Electronic Structure. The geometries of the electronic ground-state structures were optimized using Gaussian09 with the B3LYP functional²¹ and the Pople 6-311G* basis set.²² Since absorption and emission properties were measured in dichloromethane solutions, the polarizable continuum model (PCM) with dichloromethane as a solvent was employed.²³ All minimum structures were unambiguously

assigned by analytical frequency analysis. Table 5 summarizes the calculated torsional angles for pyrazoles **6a,i–p**.

Table 5. TD-DFT Calculations (CAM-B3LYP 6-311G(d,p)) of the Absorption Maxima for Pyrazoles **6a,i–p**

structure	exptl $\lambda_{\max, \text{abs}}$ ^a (nm)	calcd $\lambda_{\max, \text{abs}}$ (nm)	most dominant contributions
6a	257	250	HOMO → LUMO (44%)
			HOMO-1 → LUMO (41%)
6i	254	248	HOMO → LUMO (46%)
		235	HOMO → LUMO+1 (37%)
			HOMO-1 → LUMO (46%)
			HOMO → LUMO (19%)
6j	260	257	HOMO → LUMO (77%)
			HOMO-1 → LUMO (17%)
			HOMO → LUMO (82%)
			HOMO-1 → LUMO (13%)
6k	282	274	HOMO → LUMO (82%)
			HOMO-1 → LUMO (13%)
6l	262	257	HOMO-1 → LUMO (63%)
			HOMO → LUMO (30%)
6m	281	275	HOMO-1 → LUMO (61%)
			HOMO → LUMO (34%)
6n	280	266	HOMO-1 → LUMO (65%)
			HOMO → LUMO (14%)
			HOMO → LUMO+3 (12%)
6o	283	267	HOMO → LUMO+1 (44%)
			HOMO → LUMO+3 (32%)
			HOMO → LUMO (27%)
6p	292	281	HOMO → LUMO (46%)
		271	HOMO-1 → LUMO (46%)
			HOMO → LUMO (18%)
		HOMO → LUMO+1 (18%)	
		HOMO → LUMO+3 (17%)	

^aRecorded in dichloromethane, $T = 293$ K, $c(\mathbf{6}) = 10^{-7}$ M.

In accordance with previous results,^{9a} the calculated equilibrium ground-state structures show that the 3-aryl substituent (aryl¹) adopts an almost coplanar orientation showing angles between 5 and 8°, while the substituent at position 5 (aryl²) is distinctly twisted out of plane with torsional angles between 45 and 47°. However, upon excitation, the substituent aryl² adopts a diminished torsional angle in the excited state (Figure 5). These geometrical changes upon excitation from the ground to excited state already rationalize that in the excited state the overlap will be increased, eventually favoring delocalization and ultimately associated with a pronounced charge-transfer character. Table 6 summarizes the calculated equilibrium ground state and excited state structures for pyrazoles **6a,i–p**.

In addition, TD-DFT calculations were employed for determining and rationalizing the absorption characteristics, again applying PCM with dichloromethane as a solvent. For calculation of the absorption characteristics, the hybrid-exchange correlation functional CAM-B3LYP was implemented.²⁴ The computed results are in good agreement with measured absorption maxima. In cases where more than one excited state significantly contributes to absorption, both wavelengths are stated (Table 5).

In most cases, the computed Kohn–Sham frontier molecular orbitals show a distribution of coefficient density over the whole system in the HOMO and a shift to the acceptor-substituted aryl moiety in the LUMO. However, in the case of

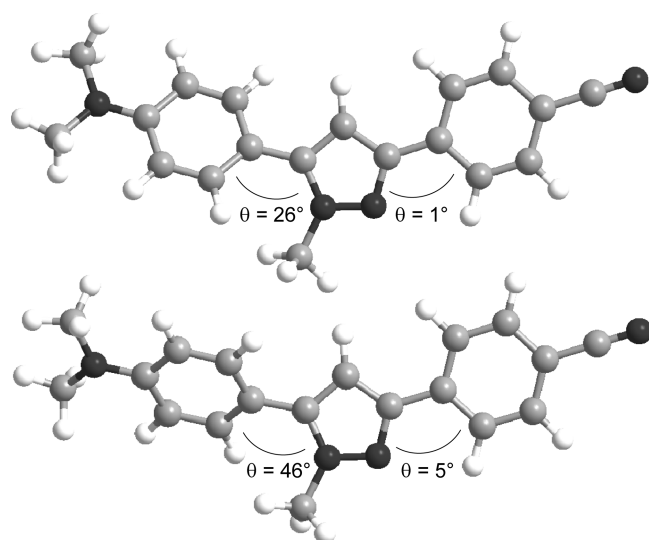


Figure 5. Optimized ground- (bottom) and excited-state (top) geometry at the B3LYP 6-311G level of DFT theory for **6p**.

Table 6. Calculated Equilibrium Ground-State and Excited-State Torsional Angles for Aryl Substituents at Position 5 (Aryl²) of Pyrazoles **6a**,*i*–**p**

structure	ground state Θ_{calc} (aryl ²) (deg)	excited state (aryl ²) (deg)
6a	47	0
6i	46	20
6j	46	24
6k	46	26
6l	47	20
6m	47	19
6n	45	22
6o	46	26
6p	46	26

dimethylamino-cyano-substituted pyrazole **6p**, transitions from HOMO to LUMO and HOMO-1 to LUMO contribute equally to the S_1 state. Both HOMO and HOMO-1 indicate a pronounced charge-transfer character, though in the HOMO the coefficient density is predominantly localized on the *p*-dimethylamino phenyl donor, whereas the HOMO-1 displays equal contributions on the pyrazole and the acceptor moiety (Figure 6). The LUMO possesses dominant coefficient density on the *p*-cyanophenyl acceptor. Therefore, the central pyrazole core, which bears substantial coefficient density in all involved frontier molecular orbitals, ensures overlap for the overall charge-transfer transition. This interpretation is in agreement with the strong solvochromicity associated with the experimentally observed large change in dipole moment. Hence, this considerable change in dipole moment rationalizes the observed enormous Stokes shift of compound **6p**.

TD-DFT calculations were also employed for the optimization of the excited-state geometry to calculate the emission characteristics. All minimum structures were unambiguously assigned by analytical frequency analysis. However, in this case, using the CAM-B3LYP functional calculated values did not reproduce the experimental values well. Upon changing the functional to B3LYP, again using PCM with dichloromethane as a solvent, a good correlation with the experimental data in dichloromethane was obtained. According to Kasha's rule, where fluorescence only occurs from the excited singlet state of

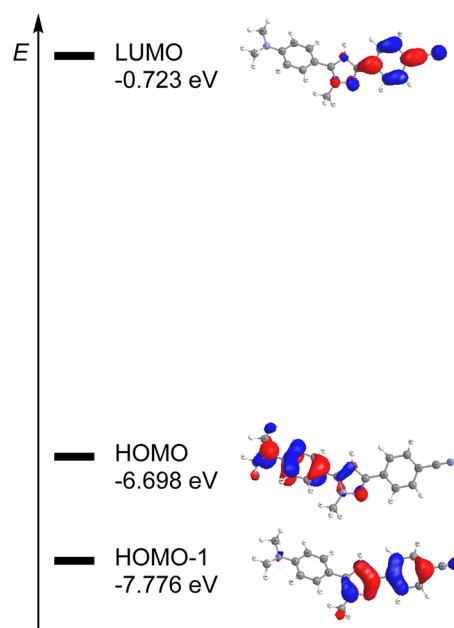


Figure 6. Selected DFT-computed (B3LYP 6-311G(d,p)) Kohn-Sham frontier molecular orbitals for **6p**.

lowest energy, only the calculated energies for S_1 states were considered for computing the emission maxima (Table 7).

Table 7. TD-DFT Calculations (B3LYP 6-311G(d,p)) of the Emission Maxima for Pyrazoles **6a**,*i*–**p**

structure	exptl $\lambda_{\text{max,Em}}$ (nm)	computed $\lambda_{\text{max,Em}}$ (nm)
6a	333	343
6i	338	337
6j	341	341
6k	348	362
6l	367	377
6m	394	402
6n	365	384
	489	
6o	448	439
6p	499	470

CONCLUSION

In conclusion, we present a novel, efficient consecutive four-component coupling-coupling-cyclocondensation synthesis of pyrazoles, taking advantage of the sequentially Pd-catalyzed one-pot generation of alkynones from aryl iodides, ethynyl-magnesium bromide, and acid chlorides. The ease of the four-component process was additionally illustrated for the one-pot synthesis of pyrimidines. The pyrazole synthesis was employed to tackle the photophysical properties of donor–acceptor substituted pyrazoles. These push–pull-substituted derivatives exhibit strongly red-shifted emission maxima with large Stokes shifts. Moreover, electronic absorption and emission spectroscopy reveals that the emission is highly solvochromic, whereas the absorption is not affected at all. The positive solvochromicity allows altering the emission color for the dimethylamino-cyano derivative in a range from 363 nm (cyclohexane) to 595 nm (acetonitrile). This feature is particularly favorable for photophysical probing of polarity environments in biological samples. In addition, the photophysical measurements were

corroborated and rationalized by accompanying state-of-the-art DFT and TD-DFT calculations. This combined methodological, physical organic study nicely illustrates that a set of structurally related luminophores can be accessed rapidly and efficiently, opening new ways to tackling biophysical and materials scientific questions by offering a practical synthetic tool. Further studies directed toward the expansion of the sequentially Pd-catalyzed entry to reactive intermediates and their implementation in physical organic studies on functional chromophores are currently underway.

EXPERIMENTAL SECTION

General Considerations. All reactions were performed in flame-dried Schlenk tubes or microwave vials under a nitrogen atmosphere. Microwave reactions were controlled and monitored with an external surface sensor. Reaction progress was monitored qualitatively by thin-layer chromatography using silica gel layered aluminum foil (F_{254}). For detection, UV light of wavelengths 254 and 366 was employed. Commercially available chemicals were used as received without any further purification. ^1H and ^{13}C NMR spectra were measured on a 300, 500, or 600 MHz spectrometer. Chemical shifts are given in ppm (δ) and were referenced to the internal solvent signal: CDCl_3 (^1H δ 7.26, ^{13}C δ 77.2) or acetone- d_6 (^1H δ 2.05, ^{13}C δ 29.8). Multiplicities are stated as s (singlet), d (doublet), t (triplet), q (quartet), m (multiplet), brs (broad singlet). Coupling constants (J) are given in Hertz. The assignment of primary (CH_3), secondary (CH_2), tertiary (CH), and quaternary carbon nuclei (C_{quat}) was made using DEPT-135 spectra. Mass spectroscopic measurements were conducted on a quadrupole (EI) or TOF (HRMS) analyzer. IR spectra were measured using ATR technique. The intensities of the IR bands are abbreviated as w (weak), m (medium), s (strong). Melting points are uncorrected.

General Procedure (GP1) for the Four-Component Synthesis of Pyrazoles 5. Bis(triphenylphosphane)palladium(II) dichloride (35.1 mg, 50.0 μmol , 5.00 mol %) and aryl iodide (1.00 mmol, 1.00 equiv, if solid) were placed in a flame-dried 10 mL microwave vial under a nitrogen atmosphere, and the vial was evacuated and flushed with nitrogen two more times. A solution of ethynylmagnesium bromide in THF (2.40 mL, 0.500 M, 1.20 mmol) was added, as was aryl iodide, if liquid. The resulting yellow solution was stirred at 45 °C to complete conversion (ca. 30 min, TLC control). Toward the end of the reaction, the mixture turned turbid. It was cooled to rt, triethylamine hydrochloride (41.3 mg, 0.300 mmol, 0.300 equiv) was added, and the mixture was stirred for several minutes before the addition of triethylamine (106 mg, 1.05 mmol, 1.05 equiv), aryl chloride (1.40 mmol, 1.40 equiv), and copper(I) iodide (9.50 mg, 50.0 μmol , 5.00 mol %), upon which the reaction mixture darkened to brown. The reaction mixture was stirred for 1–2 h at 45 °C (TLC control). After the mixture was cooled to rt, MeOH (0.400 mL), AcOH (0.400), phenanthroline (360 mg, 2.00 mmol, 2.00 equiv), and the respective hydrazine (1.50 mmol, 1.50 equiv) were added, and the mixture was heated to 150 °C for 15 min under microwave irradiation. The reaction mixture was quenched with satd aq NaHCO_3 and extracted with EtOAc (5 \times 20 mL). The combined organic phases were washed with brine and dried (MgSO_4), and the crude product was adsorbed on Celite. Purification was performed using a flash purification system with eluents consisting of *n*-hexane and EtOAc or acetone.

5-(4-Methoxyphenyl)-1-methyl-3-phenyl-1H-pyrazole (6a). According to GP1 using 4-iodoanisole, benzoyl chloride, and methyl hydrazine, 209 mg (0.775 mmol, 77%) of 6a was obtained as a yellow solid with a regioisomeric ratio of 10:1 (^1H NMR). Purification was performed with a gradient of *n*-hexane/EtOAc 19:1 \rightarrow 2:1. Mp: 108–110 °C (lit.²⁵ mp 109–110 °C). ^1H NMR (CDCl_3 , 300 MHz): δ 3.87 (s, 3 H), 3.91 (s, 3 H), 6.56 (s, 1 H), 6.98–7.03 (m, 2 H), 7.27–7.33 (m, 1 H), 7.37–7.44 (m, 4 H), 7.81–7.85 (m, 2 H). ^{13}C NMR (CDCl_3 , 75 MHz): δ 37.6 (CH_3), 55.5 (CH_3), 103.0 (CH), 114.3 (CH), 123.2 (C_{quat}), 125.6 (CH), 127.7 (CH), 128.7 (CH), 130.2 (CH), 133.7 (C_{quat}), 145.0 (C_{quat}), 150.5 (C_{quat}), 159.9 (C_{quat}). EI +

MS (m/z): 264 (100) [M^+], 249 (38) [$\text{C}_{16}\text{H}_{13}\text{N}_2\text{O}^{+\bullet}$], 176 (11), 158 (11) [$\text{C}_{10}\text{H}_8\text{NO}^{+\bullet}$], 105 (17) [$\text{C}_7\text{H}_5\text{O}^{+\bullet}$], 77 (10) [$\text{C}_6\text{H}_5^{+\bullet}$]. FT-IR: $\tilde{\nu}$ (cm^{-1}) = 606 (m), 667 (m), 677 (m), 692 (s), 745 (m), 764 (s), 799 (m), 835 (s), 957 (m), 997 (m), 1016 (m), 1028 (m), 1036 (m), 1177 (m), 1248 (s), 1290 (m), 1443 (m), 1460 (m), 1491 (s), 1612 (m), 2835 (w), 2911 (w), 2938 (w), 3001 (w), 3057 (w). Anal. Calcd for $\text{C}_{17}\text{H}_{16}\text{N}_2\text{O}$ (264.1): C, 77.25; H, 6.10; N, 10.60. Found: C, 77.03; H, 6.38; N, 10.41.

5-(4-Methoxyphenyl)-3-phenyl-1H-pyrazole (6b). According to GP1 using 4-iodoanisole, benzoyl chloride, and hydrazine hydrate, 169 mg (0.675 mmol, 68%) of 6b was obtained as a yellow solid. Purification was performed with a gradient of *n*-hexane/acetone 9:1 \rightarrow 1:1. Mp: 157–159 °C (lit.²⁶ mp 160–161 °C). ^1H NMR (CDCl_3 , 300 MHz): δ 3.74 (s, 3 H), 6.63 (s, 1 H), 6.76–6.78 (m, 2 H), 7.21–7.27 (m, 3 H), 7.53–7.55 (m, 2 H), 7.61–7.63 (m, 2 H), 11.39 (brs, 1 H). ^{13}C NMR (CDCl_3 , 75 MHz): δ 55.4 (CH_3), 99.4 (CH), 114.3 (CH), 124.0 (C_{quat}), 125.7 (CH), 127.0 (CH), 128.1 (CH), 128.8 (CH), 131.7 (C_{quat}), 148.2 (C_{quat}), 149.2 (C_{quat}), 159.6 (C_{quat}). EI + MS (m/z): 250 (100) [M^+], 235 (40) [$\text{C}_{15}\text{H}_{11}\text{N}_2\text{O}^{+\bullet}$], 207 (17) [$\text{C}_{14}\text{H}_9\text{N}_2^{+\bullet}$], 178 (13), 123 (18), 105 (31) [$\text{C}_7\text{H}_5\text{O}^{+\bullet}$], 77 (15) [$\text{C}_6\text{H}_5^{+\bullet}$]. FT-IR: $\tilde{\nu}$ (cm^{-1}) = 611 (m), 689 (s), 760 (s), 797 (m), 831 (s), 968 (m), 1028 (m), 1175 (m), 1252 (s), 1273 (m), 1300 (m), 1439 (m), 1456 (m), 1508 (m), 1614 (m), 2833 (m), 2860 (w), 2899 (w), 2934 (w), 3003 (w), 3042 (w), 3061 (w), 3111 (w). Anal. Calcd for $\text{C}_{16}\text{H}_{14}\text{N}_2\text{O}$ (250.3): C, 76.78; H, 5.64; N, 11.19. Found: C, 76.57; H, 5.72; N, 10.90.

5-(4-Chlorophenyl)-1-methyl-3-phenyl-1H-pyrazole (6c). According to GP1 using 1-chloro-4-iodobenzene, benzoyl chloride, and methyl hydrazine, 183 mg (0.680 mmol, 68%) of 6c was obtained as a light brown resin. Purification was performed with a gradient of *n*-hexane/EtOAc 19:1 \rightarrow 2:1. ^1H NMR (CDCl_3 , 300 MHz): δ 3.92 (s, 3 H), 6.60 (s, 1 H), 7.29–7.35 (m, 1 H), 7.38–7.48 (m, 6 H), 7.80–7.84 (m, 2 H). ^{13}C NMR (CDCl_3 , 75 MHz): δ 37.6 (CH_3), 103.6 (CH), 125.7 (CH), 127.9 (CH), 128.8 (CH), 129.1 (CH), 130.1 (CH), 133.3 (C_{quat}), 134.9 (C_{quat}), 144.0 (C_{quat}), 150.7 (C_{quat}), one C_{quat} not detectable due to signal overlap. EI + MS (m/z): 270 (8) [M^+ , ^{37}Cl], 268 (25) [M^+ , ^{35}Cl], 122 (96), 105 (100) [$\text{C}_7\text{H}_5\text{N}_2^{+\bullet}$], 77 (57) [$\text{C}_6\text{H}_5^{+\bullet}$], 51 (18). FT-IR: $\tilde{\nu}$ (cm^{-1}) = 667 (m), 692 (s), 712 (m), 764 (s), 799 (m), 833 (s), 957 (m), 1005 (m), 1090 (m), 1460 (m), 1481 (s), 2930 (w), 2945 (w), 2984 (w), 3057 (w), 3119 (w). HRMS (ESI) calcd for [$\text{C}_{16}\text{H}_{14}^{35}\text{ClN}_2^+$] 269.0840, found 269.0841.

5-(4-Chlorophenyl)-1-methyl-3-(*p*-tolyl)-1H-pyrazole (6d). According to GP1 using 1-chloro-4-iodobenzene, *p*-toluoyl chloride, and methyl hydrazine, 167 mg (0.590 mmol, 59%) of 6d was obtained as a yellow solid. Purification was performed with a gradient of *n*-hexane/EtOAc 19:1 \rightarrow 2:1. Mp: 100–102 °C. ^1H NMR (CDCl_3 , 300 MHz): δ 2.38 (s, 3 H), 3.91 (s, 3 H), 6.57 (s, 1 H), 7.20–7.23 (m, 2 H), 7.37–7.48 (m, 4 H), 7.69–7.73 (m, 3 H). ^{13}C NMR (CDCl_3 , 75 MHz): δ 21.4 (CH_3), 37.7 (CH_3), 103.3 (CH), 125.6 (CH), 129.1 (CH), 129.2 (C_{quat}), 129.5 (CH), 130.1 (CH), 130.5 (C_{quat}), 134.8 (C_{quat}), 137.6 (C_{quat}), 143.9 (C_{quat}), 150.8 (C_{quat}). EI + MS (m/z): 284 (100) [M^+ , ^{37}Cl], 282 (100) [M^+ , ^{35}Cl], 269 (5) [$\text{C}_{16}\text{H}_{12}^{37}\text{ClN}_2^{+\bullet}$], 267 (15) [$\text{C}_{16}\text{H}_{12}^{35}\text{ClN}_2^{+\bullet}$], 119 (18). FT-IR: $\tilde{\nu}$ (cm^{-1}) = 793 (s), 822 (m), 835 (m), 1001 (m), 1016 (m), 1088 (m), 1483 (m), 2731 (m), 2855 (w), 2913 (w), 2943 (w), 2963 (w), 3017 (w), 3051 (w). HRMS (ESI): calcd for [$\text{C}_{17}\text{H}_{16}^{35}\text{ClN}_2^+$] 283.0997, found 283.0995.

5-(4-Chlorophenyl)-3-phenyl-1H-pyrazole (6e). According to GP1 using 1-chloro-4-iodobenzene, benzoyl chloride, and hydrazine hydrate, 163 mg (0.640 mmol, 64%) of 6e was obtained as a colorless solid. Purification was performed with a gradient of *n*-hexane/EtOAc 19:1 \rightarrow 2:1. Mp: 214–215 °C (lit.²⁷ mp 216–217 °C). ^1H NMR (acetone- d_6 , 600 MHz): δ 7.15 (s, 1 H), 7.35–7.38 (m, 1 H), 7.45–7.48 (m, 4 H), 7.86–7.88 (m, 2 H), 7.90–7.92 (m, 2 H). NH not visible due to quick exchange. ^{13}C NMR (acetone- d_6 , 150 MHz): δ 100.6 (CH), 126.2 (CH), 127.8 (CH), 128.9 (CH), 129.65 (CH), 129.73 (CH), 133.7 (C_{quat}). Other C_{quat} not detectable due to aggregation effects. EI + MS (m/z): 254 (100) [M^+], 225 (11) [$\text{C}_{15}\text{H}_{10}^{35}\text{Cl}^{+\bullet}$], 189 (15), 94 (15). FT-IR: $\tilde{\nu}$ (cm^{-1}) = 662 (m), 677 (s), 739 (m), 756 (s), 793 (m), 824 (s), 974 (m), 1011 (m), 1061 (m), 1086 (m), 1096 (m), 1456 (m), 1477 (m), 2729 (w), 2762 (w),

2797 (w), 2841 (w), 2857 (w), 2868 (w), 2920 (w), 2980 (w); 3005 (w), 3065 (w), 3100 (w), 3144 (w), 3194 (w), 3746 (w). Anal. Calcd for $C_{15}H_{11}ClN_2$ (254.7): C, 70.73; H, 4.35; N, 11.00. Found: C, 71.02; H, 4.37; N, 10.73.

1-Methyl-5-phenyl-3-(*p*-tolyl)-1H-pyrazole (6f). According to GP1 using iodobenzene, *p*-toluoyl chloride, and methyl hydrazine, 196 mg (0.789 mmol, 79%) of **6f** was obtained as a yellow solid. Purification was performed with a gradient of *n*-hexane/EtOAc 19:1 → 2:1. Mp: 125–126 °C (lit.²⁵ mp 129–131 °C). 1H NMR ($CDCl_3$, 300 MHz): δ 2.38 (s, 3 H), 3.93 (s, 3 H), 6.59 (s, 1 H), 7.21–7.24 (s, 2 H), 7.37–7.49 (m, 5 H), 7.71–7.75 (m, 2 H). ^{13}C NMR ($CDCl_3$, 75 MHz): δ 21.4 (CH_3), 37.7 (CH_3), 103.2 (CH), 125.6 (CH), 128.6 (CH), 128.8 (CH), 128.9 (CH), 129.5 (CH), 130.8 (C_{quat}), 130.9 (C_{quat}), 137.5 (C_{quat}), 145.1 (C_{quat}), 150.7 (C_{quat}). EI + MS (m/z): 248 (100) [M^+], 233 (12) [$C_{16}H_{13}N_2^{+}$]. FT-IR: $\tilde{\nu}$ (cm^{-1}) = 669 (m), 696 (s), 768 (s), 799 (s), 829 (s), 1485 (m), 2735 (w), 2832 (w); 2857 (w), 2918 (w), 2945 (w), 2994 (w), 3021 (w), 3119 (w). Anal. Calcd for $C_{17}H_{16}N_2$ (248.3): C, 82.22; H, 6.49; N, 11.28. Found: C, 81.97; H, 6.48; N, 11.15.

1-Methyl-5-(naphthalen-2-yl)-3-phenyl-1H-pyrazole (6g). Deviating from GP1, the reaction was performed on a 0.880 mmol scale. Using 2-iodonaphthalene, benzoyl chloride, and methyl hydrazine, 176 mg (0.619 mmol, 70%) of **6g** was obtained as a yellow resin. Purification was performed with a gradient of *n*-hexane/EtOAc 19:1 → 2:1. 1H NMR ($CDCl_3$, 300 MHz): δ 4.01 (s, 3 H), 6.72 (s, 1 H), 7.30–7.36 (m, 2 H), 7.40–7.46 (m, 3 H), 7.85–7.97 (m, 6 H). ^{13}C NMR ($CDCl_3$, 75 MHz): δ 37.9 (CH_3), 103.7 (CH), 125.7 (CH), 126.4 (CH), 126.9 (CH), 127.8 (CH), 127.9 (CH), 128.1 (CH), 128.1 (C_{quat}), 128.3 (CH), 128.6 (CH), 128.8 (CH), 133.1 (C_{quat}), 133.2 (C_{quat}), 133.6 (C_{quat}), 145.2 (C_{quat}), 150.8 (C_{quat}). EI + MS (m/z): 284 (100) [M^+], 153 (11) [$C_{11}H_7N^{+}$]. FT-IR: $\tilde{\nu}$ (cm^{-1}) = 669 (m), 692 (s), 737 (m), 750 (s), 762 (s), 797 (m), 820 (m), 860 (m), 959 (m), 1458 (m), 2803 (w), 2945 (w), 2984 (w), 3022 (w), 3053 (w). HRMS (ESI): calcd for [$C_{20}H_{17}N_2^+$] 285.1386, found 285.1389.

1-Methyl-3-phenyl-5-(4-(trifluoromethoxy)phenyl)-1H-pyrazole (6h). According to GP1 using 1-iodo-4-trifluoromethoxyiodobenzene, benzoyl chloride, and methyl hydrazine, 186 mg (0.584 mmol, 58%) of **6h** was obtained as a beige solid. Purification was performed with a gradient of *n*-hexane/EtOAc 19:1 → 2:1. Mp: 135–137 °C. 1H NMR ($CDCl_3$, 300 MHz): δ 3.93 (s, 3 H), 6.61 (s, 1 H), 7.31–7.34 (m, 3 H), 7.40–7.43 (m, 2 H), 7.49–7.51 (m, 2 H), 7.82–7.84 (m, 2 H). ^{13}C NMR ($CDCl_3$, 75 MHz): δ 37.7 (CH_3), 103.7 (CH), 120.6 (q, C_{quat} $^1J_{HF}$ = 259 Hz), 121.3 (CH), 125.7 (CH), 127.9 (CH), 128.8 (CH), 129.5 (C_{quat}), 130.4 (CH), 133.3 (C_{quat}), 143.8 (C_{quat}), 149.5 (C_{quat}), 150.8 (C_{quat}). EI + MS (m/z): 318 (100) [M^+], 202 (5) [$C_6H_7F_3NO^{+}$]. FT-IR: $\tilde{\nu}$ (cm^{-1}) = 658 (m), 692 (s), 764 (s), 799 (m), 854 (m), 1005 (m), 1107 (m), 1161 (s), 1204 (s), 1252 (s), 1491 (m), 2853 (w), 2884 (w), 2924 (w), 2957 (w), 3061 (w). Anal. Calcd for $C_{17}H_{13}F_3N_2O$ (318.3): C, 64.15; H, 4.12; N, 8.80. Found: C, 63.94; H, 4.27; N, 8.50.

1-Methyl-3,5-diphenyl-1H-pyrazole (6i). According to GP1 using iodobenzene, benzoyl chloride, and methyl hydrazine, 168 mg (0.717 mmol, 72%) of **6i** was obtained as a yellow resin which crystallized over several weeks. Purification was performed with a gradient of *n*-hexane/EtOAc 19:1 → 4:1. 1H NMR ($CDCl_3$, 300 MHz): δ 3.94 (s, 3 H), 6.62 (s, 1 H), 7.28–7.34 (m, 1 H), 7.39–7.50 (m, 7 H), 7.82–7.86 (m, 2 H). ^{13}C NMR ($CDCl_3$, 75 MHz): δ 37.7 (CH_3), 103.4 (CH), 125.7 (CH), 127.7 (CH), 128.7 (CH), 128.8 (CH), 128.8 (CH), 128.9 (CH), 130.8 (C_{quat}), 133.6 (C_{quat}), 145.2 (C_{quat}), 150.6 (C_{quat}). EI + MS (m/z): 234 (100) [M^+], 77 (10) [$C_6H_5^{+}$]. FT-IR: $\tilde{\nu}$ (cm^{-1}) = 671 (m), 691 (s), 746 (s), 762 (s), 1485 (m), 2943 (w), 2986 (w), 3044 (w), 3059 (w), 3119 (w). Anal. Calcd for $C_{16}H_{14}N_2$ (234.3): C, 82.02; H, 6.02; N, 11.96. Found: C, 82.10; H, 5.91; N, 11.72.

1-Methyl-3-phenyl-5-(4-(trifluoromethyl)phenyl)-1H-pyrazole (6j). According to GP1 using iodobenzene, 4-(trifluoromethyl)benzoyl chloride, and methyl hydrazine, 133 mg (0.440 mmol, 44%) of **6j** was obtained as a light yellow solid. Purification was performed twice with gradients of *n*-hexane/EtOAc 5:1 → 2:1 and 19:1 → 9:1, respectively, followed by manual flash chromatography (*n*-hexane/EtOAc 40:1). Mp: 76–77 °C. 1H NMR ($CDCl_3$, 300 MHz): δ 3.95 (s, 3 H), 6.66 (s,

1 H), 7.44–7.50 (m, 5 H), 7.64–7.67 (m, 2 H), 7.92–7.96 (m, 2 H). ^{13}C NMR ($CDCl_3$, 75 MHz): δ 37.9 (CH_3), 103.8 (CH), 124.4 (q, C_{quat} 1J_F = 273 Hz), 125.7 (CH), 125.7 (q, CH, 3J_F = 4 Hz), 128.9 (CH), 128.9 (CH), 128.9 (CH), 129.5 (q, C_{quat} 2J_F = 32 Hz), 130.5 (C_{quat}), 137.0 (q, C_{quat} 5J_F = 1 Hz), 145.6 (C_{quat}), 149.1 (C_{quat}). EI + MS (m/z): 302 (28) [M^+], 173 (100) [$C_8H_6F_3N_2^{+}$], 145 (31) [$C_7H_4F_3^{+}$], 114 (12) [$C_8H_4N^{+}$], 71 (17), 54 (46) [$C_3H_4N^{+}$], 43 (47) [$CH_3N_2^{+}$]. FT-IR: $\tilde{\nu}$ (cm^{-1}) = 671 (m), 692 (m), 768 (s), 800 (m), 839 (m), 853 (m), 959 (m), 1007 (m), 1043 (m), 1063 (s), 1107 (s), 1159 (m), 1182 (m), 1238 (m), 1275 (m), 1323 (s), 2859 (w), 2938 (w), 2955 (w), 2988 (w), 3082 (w). HRMS (ESI): calcd for [$C_{17}H_{14}F_3N_2^+$] 303.1104, found 303.1109.

4-(1-Methyl-5-phenyl-1H-pyrazol-3-yl)benzotrile (6k). According to GP1 using iodobenzene, 4-cyanobenzoyl chloride, and methyl hydrazine, 91 mg (0.350 mmol, 35%) of **6k** was obtained as a colorless solid. Purification was performed with a gradient of *n*-hexane/EtOAc 19:1 → 2:1, an analytical sample for photophysical characterization was recrystallized from *n*-hexane. Mp: 141–143 °C. 1H NMR ($CDCl_3$, 300 MHz): δ 3.94 (s, 3 H), 6.66 (s, 1 H), 7.42–7.53 (m, 5 H), 7.66–7.70 (m, 2 H), 7.91–7.95 (m, 2 H). ^{13}C NMR ($CDCl_3$, 75 MHz): δ 38.0 (CH_3), 104.0 (CH), 110.9 (C_{quat}), 119.3 (C_{quat}), 125.9 (CH), 128.9 (CH), 128.97 (CH), 129.02 (CH), 130.3 (CH), 132.7 (CH), 138.0 (C_{quat}), 145.7 (C_{quat}), 148.6 (C_{quat}). One C_{quat} not detectable due to signal overlap. EI + MS (m/z): 259 (32) [M^+], 130 (100) [$C_{10}H_{10}^{+}$], 114 (11) [$C_8H_4N^{+}$], 102 (29) [$C_7H_4N^{+}$], 71 (23), 54 (60) [$C_3H_4N^{+}$], 43 (65) [$CH_3N_2^{+}$]. FT-IR: $\tilde{\nu}$ (cm^{-1}) = 691 (m), 702 (m), 766 (s), 770 (m), 847 (m), 957 (m), 1007 (m), 1022 (m), 1059 (m), 1109 (m), 1128 (m), 1179 (m), 1248 (m), 1260 (m), 1283 (m), 2882 (w), 2909 (w), 2949 (w). HRMS (ESI): calcd for [$C_{17}H_{14}N_3^+$] 260.1182, found 260.1181.

5-(4-Methoxyphenyl)-1-methyl-3-(4-trifluoromethyl)phenyl)-1H-pyrazole (6l). According to GP1 using 4-iodoanisole, 4-(trifluoromethyl)benzoyl chloride, and methyl hydrazine, 192 mg (0.577 mmol, 58%) of **6l** was obtained as a light yellow solid. Purification was performed with a gradient of *n*-hexane/EtOAc 19:1 → 2:1, and an analytical sample for photophysical characterization was recrystallized from *n*-hexane. Mp: 110–112 °C. 1H NMR ($CDCl_3$, 300 MHz): δ 3.87 (s, 3 H), 3.92 (s, 3 H), 6.60 (s, 1 H), 6.99–7.03 (m, 2 H), 7.37–7.40 (m, 2 H), 7.63–7.67 (m, 2 H), 7.91–7.95 (m, 2 H). ^{13}C NMR ($CDCl_3$, 75 MHz): δ 37.8 (CH_3), 55.5 (CH_3), 103.5 (C_{quat}), 114.4 (CH), 124.5 (q, C_{quat} 1J_F = 272 Hz), 122.8 (CH), 125.67 (CH), 125.70 (q, CH, 3J_F = 4 Hz), 130.2 (CH), 137.1 (q, C_{quat} 5J_F = 1 Hz), 145.4 (C_{quat}), 149.1 (C_{quat}), 160.1 (C_{quat}). EI + MS (m/z): 332 (100) [M^+], 317 (32) [$C_{17}H_{12}F_3N_2O^{+}$]. FT-IR: $\tilde{\nu}$ (cm^{-1}) = 608 (m), 633 (m), 675 (m), 770 (m), 791 (s), 833 (s), 849 (s), 959 (m), 999 (m), 1015 (m), 1038 (m), 1065 (s), 1090 (m), 1111 (s), 1161 (s), 1177 (m), 1252 (s), 1292 (m), 1321 (s), 1425 (m), 1447 (m), 1462 (m), 1495 (m), 1614 (m), 2841 (w), 2886 (w), 2909 (w), 2936 (w), 2967 (w), 3076 (w). Anal. Calcd for $C_{18}H_{15}F_3N_2O$ (332.3): C, 65.06; H, 4.55; N, 8.43. Found: C, 65.33; H, 4.72; N, 8.19.

4-(5-(4-Methoxyphenyl)-1-methyl-1H-pyrazol-3-yl)benzotrile (6m). According to GP1 using 4-iodoanisole, 4-cyanobenzoyl chloride, and methyl hydrazine, 125 mg (0.432 mmol, 43%) of **6m** was obtained as a colorless solid. Purification was performed with a gradient of *n*-hexane/EtOAc 19:1 → 2:1. An analytical sample for photophysical characterization was recrystallized from *n*-hexane. Mp: 161–162 °C. 1H NMR ($CDCl_3$, 300 MHz): δ 3.87 (s, 3 H), 3.91 (s, 3 H), 6.60 (s, 1 H), 7.01 (m, 2 H), 7.37 (m, 2 H), 7.67 (m, 2 H), 7.91 (m, 2 H). ^{13}C NMR ($CDCl_3$, 75 MHz): δ 37.8 (CH_3), 55.5 (CH_3), 103.6 (CH), 110.7 (C_{quat}), 114.4 (CH), 119.3 (C_{quat}), 122.6 (C_{quat}), 125.9 (CH), 130.2 (CH), 132.6 (CH), 138.1 (C_{quat}), 145.5 (C_{quat}), 148.5 (C_{quat}), 160.2 (C_{quat}). EI + MS (m/z): 289 (100) [M^+], 274 (29) [$C_{17}H_{12}N_3O^{+}$]. FT-IR: $\tilde{\nu}$ (cm^{-1}) = 613 (m), 677 (m), 712 (m), 768 (s), 812 (m), 827 (s), 841 (m), 1001 (m), 1013 (m), 1030 (m), 1111 (m), 1177 (s), 1254 (s), 1296 (m), 1423 (m), 1445 (m), 1468 (m), 1491 (s), 1611 (m), 2226 (m), 2847 (w), 2911 (w), 2953 (w), 2982 (w), 3044 (w). HRMS (ESI): calcd for [$C_{18}H_{16}N_3O^+$] 290.1288, found 290.1290.

***N,N*-Dimethyl-4-(1-methyl-3-phenyl-1H-pyrazol-5-yl)aniline (6n).** According to GP1 using 4-iodo-*N,N*-dimethylaniline, benzoyl chloride,

and methyl hydrazine, 180 mg (0.595 mmol, 60%) of **6n** was obtained as a light brown resin. Purification was performed with a gradient of *n*-hexane/EtOAc 4:1 → 1:1. ¹H NMR (CDCl₃, 300 MHz): δ 3.02 (s, 6 H), 3.93 (s, 3 H), 6.54 (s, 1 H), 6.77–6.82 (m, 2 H), 7.27–7.44 (m, 5 H), 7.82–7.85 (m, 2 H). ¹³C NMR (CDCl₃, 75 MHz): δ 37.6 (CH₃), 40.5 (CH₃), 102.6 (CH), 112.2 (CH), 118.3 (CH), 125.6 (CH), 127.5 (C_{quat}), 128.7 (CH), 129.7 (CH), 133.8 (C_{quat}), 145.7 (C_{quat}), 150.4 (C_{quat}), 150.5 (C_{quat}). EI + MS (*m/z*): 277 (23) [M⁺], 158 (100) [C₁₀H₁₀N₂⁺], 130 (19), 205 (30), 103 (10), 77 (22) [C₆H₅⁺], 43 (22) [CH₃N₂⁺]. FT-IR: $\tilde{\nu}$ (cm⁻¹) = 667 (m), 675 (m), 692 (s), 762 (s), 797 (m), 820 (m), 945 (m), 957 (m), 1167 (m), 1188 (m), 1227 (m), 1360 (s), 1445 (m), 1460 (m), 1495 (s), 1522 (m), 1612 (m), 2725 (w), 2805 (w), 2855 (w), 2887 (w), 2980 (w), 3034 (w), 3055 (w). HRMS (ESI): calcd for [C₁₈H₂₀N₃⁺] 278.1652, found 278.1652.

N,N-Dimethyl-4-(1-methyl-3-(4-(trifluoromethyl)phenyl)-1H-pyrazol-5-yl)aniline (**6o**). According to GP1 using 4-iodo-*N,N*-dimethylaniline, 4-(trifluoromethyl)benzoyl chloride, and methyl hydrazine, 180 mg (0.576 mmol, 58%) of **6o** was obtained as a light yellow solid. Purification was performed with a gradient of *n*-hexane/acetone 19:1 → 2:1, an analytical sample for photophysical characterization was recrystallized from *n*-hexane. Mp: 150–152 °C. ¹H NMR (CDCl₃, 300 MHz): δ 3.03 (s, 6 H), 3.93 (s, 3 H), 6.57 (s, 1 H), 6.77–6.82 (m, 2 H), 7.31–7.36 (m, 2 H), 7.63–7.66 (m, 2 H), 7.92–7.95 (m, 2 H). ¹³C NMR (CDCl₃, 75 MHz): δ 37.8 (CH₃), 40.5 (CH₃), 102.2 (CH), 112.2 (CH), 117.9 (C_{quat}), 124.5 (q, C_{quat}, ¹J_F = 272 Hz), 125.66 (CH), 125.69 (q, CH, ³J_F = 4 Hz), 129.3 (q, C_{quat}, ²J_F = 32.2 Hz), 129.7 (CH), 137.3 (C_{quat}), 146.1 (C_{quat}), 149.0 (C_{quat}), 150.6 (C_{quat}). EI + MS (*m/z*): 345 (100) [M⁺], 172 (25) [C₈H₅F₃N⁺]. FT-IR: $\tilde{\nu}$ (cm⁻¹) = 779 (m), 841 (m), 851 (m), 945 (m), 959 (m), 1013 (m), 1063 (m), 1092 (m), 1109 (s), 1155 (m), 1292 (m), 1323 (m), 1497 (m), 1609 (m), 2714 (w), 2810 (w), 2862 (w), 2901 (w), 2928 (w), 2999 (w), 3030 (w). Anal. Calcd for C₁₉H₁₈F₃N₃ (345.4): C, 66.08; H, 5.25; N, 12.17. Found: C, 66.18; H, 4.99; N, 12.08.

4-(5-(4-(Dimethylamino)phenyl)-1-methyl-1H-pyrazol-3-yl)benzonitrile (**6p**). According to GP1 using 4-iodo-*N,N*-dimethylaniline, 4-cyanobenzoyl chloride, and methyl hydrazine, 180 mg (0.595 mmol, 60%) of **6p** was obtained as a colorless solid. Purification was performed with a gradient of *n*-hexane/EtOAc 19:1 → 9:1, and an analytical sample for photophysical characterization was recrystallized from *n*-hexane. Mp: 187–188 °C. ¹H NMR (CDCl₃, 300 MHz): δ 3.30 (s, 6 H), 3.93 (s, 3 H), 6.57 (s, 1 H), 6.78–6.81 (m, 2 H), 7.29–7.34 (m, 2 H), 7.65–7.69 (m, 2 H), 7.90–7.94 (m, 2 H). ¹³C NMR (CDCl₃, 75 MHz): δ 37.9 (CH₃), 40.5 (CH₃), 103.2 (CH), 110.7 (C_{quat}), 112.2 (CH), 117.6 (C_{quat}), 119.4 (C_{quat}), 125.9 (CH), 129.7 (CH), 132.6 (CH), 138.3 (C_{quat}), 146.3 (C_{quat}), 148.4 (C_{quat}), 150.7 (C_{quat}). EI + MS (*m/z*): 302 (100) [M⁺], 151 (20). FT-IR: $\tilde{\nu}$ (cm⁻¹) = 673 (m), 716 (m), 729 (m), 764 (m), 777 (s), 822 (s), 845 (s), 947 (m), 1016 (m), 1038 (m), 1072 (m), 1090 (m), 1117 (m), 1125 (m), 1175 (m), 1233 (m), 1277 (m), 1300 (m), 1325 (m), 1358 (m), 1422 (m), 1445 (m), 1470 (m), 1470 (m), 1526 (m), 1607 (m), 2220 (m), 2812 (w), 2866 (w), 2899 (w), 2992 (w), 3030 (w), 3048 (w), 3073 (w), 3215 (w). Anal. Calcd for C₁₉H₁₈N₄ (302.5): C, 75.47; H, 6.00; N, 18.53. Found: C, 75.28; H, 5.98; N, 18.23.

3-(4-Methoxyphenyl)-1,5-diphenyl-1H-pyrazole (**6q**). Deviating from GP1 using 4-iodoanisole, benzoyl chloride, and phenyl hydrazine, the reaction time for the cyclization was prolonged to 45 min. After purification with a gradient of *n*-hexane/EtOAc 19:1 → 2:1, 153 mg (0.469 mmol, 47%) of **6q** was obtained as a yellow resin with a regioisomeric ratio of 1:2. An analytical sample was precipitated by immersion of an *n*-hexane solution in an ultrasonic bath, which gave **6q** as a single regioisomer. ¹H NMR (CDCl₃, 500 MHz): δ 3.86 (s, 3 H), 6.76 (s, 1 H), 6.96–6.99 (m, 2 H), 7.28–7.38 (m, 10 H), 7.85–7.87 (m, 2 H). ¹³C NMR (CDCl₃, 125 MHz): δ 55.5 (CH₃), 105.0 (CH), 114.3 (CH), 125.5 (CH), 126.1 (C_{quat}), 127.3 (CH), 127.4 (CH), 128.4 (CH), 128.6 (CH), 128.9 (CH), 129.0 (CH), 131.0 (C_{quat}), 140.4 (C_{quat}), 144.5 (C_{quat}), 152.0 (C_{quat}), 159.8 (C_{quat}). EI + MS (*m/z*): 326 (100) [M⁺], 311 (20) [C₂₁H₁₅N₂O⁺]. FT-IR: $\tilde{\nu}$ (cm⁻¹) = 677 (m), 692 (s), 760 (s), 804 (m), 840 (m), 955 (m), 972 (m), 1028 (m), 1065 (m), 1252 (m), 1431 (m), 1452 (m), 1487 (m),

1501 (m), 2841 (w), 2974 (w), 3007 (w), 3057 (w). HRMS (ESI): calcd for [C₂₂H₁₉N₂O⁺] 327.1492, found 327.1498.

1,4-Bis(1-methyl-3-phenyl-1H-pyrazol-5-yl)benzene (**6r**). Deviating from GP1, 1.00 equiv of 1,4-diiodobenzene was used, and the amounts of all other reactants and catalysts were doubled, using benzoyl chloride and methyl hydrazine. Compound **6r** (223 mg (0.571 mmol, 57%) was obtained as a yellow solid. Purification was performed with a gradient of *n*-hexane/EtOAc 19:1 → 2:1. Mp: 227–229 °C. ¹H NMR (CDCl₃, 300 MHz): δ 4.00 (s, 6 H), 6.68 (s, 2 H), 7.30–7.36 (m, 4 H), 7.41–7.46 (m, 4 H), 7.59 (s, 4 H), 7.84–7.87 (m, 4 H). ¹³C NMR (CDCl₃, 75 MHz): δ 37.9 (CH₃), 103.7 (CH), 125.7 (CH), 127.9 (CH), 128.8 (CH), 129.1 (CH), 130.9 (C_{quat}), 133.4 (C_{quat}), 144.4 (C_{quat}), 150.8 (C_{quat}). EI + MS (*m/z*): 390 (100) [M⁺], 195 (16). FT-IR: $\tilde{\nu}$ (cm⁻¹) = 667 (m), 692 (s), 766 (s), 804 (m), 851 (m), 1005 (m), 1460 (m), 2803 (w), 2926 (w), 2951 (w), 3032 (w), 3063 (w), 3130 (w). HRMS (ESI): calcd for [C₂₆H₂₃N₄⁺] 391.1917, found 391.1920.

General Procedure (GP2) for the Four-Component Synthesis of Pyrimidines 8. Bis(triphenylphosphane)palladium(II) dichloride (35.1 mg, 50.0 μmol, 5.00 mol %) and aryl iodide (1.00 mmol, 1.00 equiv, if solid) were placed in a flame-dried 20 mL Schlenk tube under a nitrogen atmosphere, and the vial was evacuated and flushed with nitrogen two more times. A solution of ethynylmagnesium bromide in THF (2.40 mL, 0.500 mmol, 1.20 mmol, 1.20 equiv) was added, as was aryl iodide, if liquid. The resulting yellow solution was stirred at 45 °C until complete conversion (ca. 30 min, TLC control). Toward the end of the reaction the mixture turned turbid. The mixture was cooled to rt, triethylamine hydrochloride (41.3 mg, 0.300 mmol, 0.300 equiv) was added, and the mixture was stirred for several minutes before the addition of triethylamine (106 mg, 1.05 mmol, 1.05 equiv), aryl chloride (1.40 mmol, 1.40 equiv), and copper(I) iodide (9.50 mg, 50.0 μmol, 5.00 mol %), upon which the reaction mixture darkened to brown. The reaction mixture was stirred for 1–2 h at 45 °C (TLC control). After the mixture was cooled to rt, THF (2.60 mL), 2-methoxyethanol (2.00 mL) and a solution of benzamide-HCl (392 mg, 2.50 mmol, 2.50 equiv) and K₂CO₃ (346 mg, 2.50 mmol, 2.50 equiv) in H₂O (1.50 mL) were added, and the mixture was heated to 90 °C for 16 h in a preheated oil bath. The reaction mixture was quenched with satd aq NH₄Cl and extracted with EtOAc (3 × 20 mL). The combined organic phases were washed with brine and dried (MgSO₄), and the crude product was adsorbed on celite. Purification was performed using a flash purification system (*n*-hexane/acetone 19:1) followed by recrystallization from *n*-hexane, if necessary.

4-(4-Methoxyphenyl)-2,6-diphenylpyrimidine (**8a**). According to GP2 using 4-iodoanisole and benzoyl chloride, 171 mg (0.505 mmol, 51%) of **8a** was obtained as a colorless solid. Purification was performed using the flash purification system. Mp: 140–142 °C (lit.²⁸ mp 138–140 °C). ¹H NMR (CDCl₃, 600 MHz): δ 3.90 (s, 3 H), 7.06–7.08 (m, 2 H), 7.51–7.58 (m, 6 H), 7.94 (s, 1 H), 8.27–8.39 (m, 4 H), 8.73–8.74 (m, 2 H). ¹³C NMR (CDCl₃, 75 MHz): δ 55.6 (CH₃), 109.5 (CH), 114.4 (CH), 127.4 (CH), 128.5 (CH), 128.6 (CH), 128.9 (CH), 129.0 (CH), 130.1 (C_{quat}), 130.7 (CH), 130.8 (CH), 137.8 (C_{quat}), 138.4 (C_{quat}), 162.0 (C_{quat}), 164.3 (C_{quat}), 164.5 (C_{quat}), 164.6 (C_{quat}). EI + MS (*m/z*): 338 (100) [M⁺], 235 (21) [C₁₆H₁₃NO⁺], 220 (32) [C₁₈H₁₂NO⁺], 132 (11), 102 (10) [C₇H₅N₂⁺]. FT-IR: $\tilde{\nu}$ (cm⁻¹) = 689 (s), 731 (m), 752 (s), 773 (m), 829 (s), 1026 (m), 1171 (s), 1236 (m), 1256 (m), 1366 (s), 1495 (m), 1512 (s), 1526 (s), 1566 (s), 1587 (m), 1609 (m), 2841 (w), 2951 (w), 3005 (w), 3034 (w). Anal. Calcd for C₂₃H₁₈N₂O (338.4): C, 81.63; H, 5.36; N, 8.28. Found: C, 81.60; H, 5.60; N, 8.02.

2,4-Diphenyl-6-(*p*-tolyl)pyrimidine (**8b**). According to GP2 using 4-iodotoluene and benzoyl chloride, 138 mg (0.428 mmol, 43%) of **8b** was obtained as colorless crystals. Purification was performed using the flash purification system, followed by recrystallization of the impure fractions from *n*-hexane (5 mL). Mp: 149–150 °C (lit.²⁹ mp 148–150 °C). ¹H NMR (CDCl₃, 600 MHz): δ 2.47 (s, 3 H), 7.35–7.39 (m, 2 H), 7.50–7.61 (m, 6 H), 7.99 (s, 1 H), 8.19–8.23 (m, 2 H), 8.27–8.32 (m, 2 H), 8.72–8.77 (m, 2 H). ¹³C NMR (CDCl₃, 75 MHz): δ 21.6 (CH₃), 110.1 (CH), 127.3 (CH), 127.4 (CH), 128.55 (CH), 128.60 (CH), 129.0 (CH), 129.8 (CH), 130.7 (CH), 130.8 (CH), 134.9

(C_{quat}), 137.8 (C_{quat}), 138.4 (C_{quat}), 141.3 (C_{quat}), 164.6 (C_{quat}), 164.7 (C_{quat}), 164.8 (C_{quat}). EI + MS (*m/z*): 322 (100) [M⁺], 219 (79) [C₁₅H₁₁N₂⁺], 204 (48) [C₁₆H₁₂⁺], 115 (32) [C₈H₅N⁺], 102 (31) [C₇H₄N⁺]. FT-IR: $\tilde{\nu}$ (cm⁻¹) = 631 (s), 642 (m), 664 (s), 685 (s), 718 (m), 746 (s), 773 (m), 824 (m), 1016 (m), 1070 (m), 1171 (m), 1236 (m), 1360 (s), 1497 (m), 1510 (s), 1522 (s), 1566 (s), 1589 (m), 2918 (w), 2990 (w), 3030 (w), 3057 (w). Anal. Calcd for C₂₃H₁₈N₂ (322.41): C, 85.68; H, 5.63; N, 8.69. Found: C, 85.83; H, 5.33; N, 8.49.

4-(Naphthalen-2-yl)-2-phenyl-6-(*p*-tolyl)pyrimidine (8c). According to GP2 using 2-iodonaphthalene and *p*-toluoyl chloride, 170 mg (0.456 mmol, 46%) of **8c** was obtained as light yellow crystals. Purification was performed using the flash purification system, followed by recrystallization from *n*-hexane (15 mL). Mp: 153–155 °C. ¹H NMR (CDCl₃, 600 MHz): δ 2.48 (s, 3 H), 7.37–7.40 (m, 2 H), 7.50–7.61 (m, 5 H), 7.90–7.95 (m, 1 H), 8.00–8.06 (m, 2 H), 8.12–8.13 (m, 1 H), 8.23–8.26 (m, 2 H), 8.38–8.42 (m, 1 H), 8.76–8.80 (m, 3 H). ¹³C NMR (CDCl₃, 75 MHz): δ 21.7 (CH₃), 110.3 (CH), 124.4 (CH), 126.7 (CH), 127.36 (CH), 127.39 (CH), 127.5 (CH), 127.9 (CH), 128.6 (CH), 128.7 (CH), 128.8 (CH), 129.2 (CH), 129.8 (CH), 130.7 (CH), 133.5 (C_{quat}), 134.7 (C_{quat}), 134.9 (C_{quat}), 135.1 (C_{quat}), 138.4 (C_{quat}), 141.3 (C_{quat}), 164.6 (C_{quat}), 164.8 (C_{quat}). One C_{quat} not detectable due to signal overlap. EI + MS (*m/z*): 372 (100) [M⁺], 269 (45) [C₂₀H₁₅N⁺], 254 (34) [C₂₀H₁₄⁺], 167 (11) [C₁₂H₉N⁺], 152 (27), 149 (42), 115 (19), 97 (11), 85 (11), 83 (11), 71 (21), 57 (37). FT-IR: $\tilde{\nu}$ (cm⁻¹) = 613 (m), 660 (m), 692 (s), 746 (s), 756 (s), 816 (s), 853 (m), 885 (m), 1016 (m), 1115 (m), 1339 (m), 1371 (m), 1435 (m), 1506 (m), 1531 (s), 1568 (m), 1589 (m), 2918 (w), 2972 (w), 3022 (w). Anal. Calcd for C₂₇H₂₀N₂ (372.5): C, 87.07; H, 5.41; N, 7.52. Found: C, 87.04; H, 5.16; N, 7.53.

2,4-Diphenyl-6-(4-(trifluoromethyl)phenyl)pyrimidine (8d). According to GP2 using 4-iodobenzotrifluoride and benzoyl chloride, 157 mg (0.417 mmol, 42%) of **8d** was obtained as colorless crystals. Purification was performed using the flash purification system, followed by recrystallization from *n*-hexane (9 mL). Mp: 147–149 °C. ¹H NMR (CDCl₃, 600 MHz): δ 7.53–7.60 (m, 6 H), 7.81–7.82 (m, 2 H), 8.00 (s, 1 H), 8.28–8.31 (m, 2 H), 8.37–8.38 (m, 2 H), 8.70–8.74 (m, 2 H). ¹³C NMR (CDCl₃, 150 MHz): δ 110.7 (CH), 124.1 (q, C_{quat}, ¹J_F = 272 Hz), 126.0 (q, CH, ³J_F = 4 Hz), 127.4 (CH), 127.8 (CH), 128.6 (CH), 128.7 (CH), 129.1 (CH), 131.0 (CH), 131.2 (CH), 132.5 (q, C_{quat}, ²J_F = 33 Hz), 137.3 (C_{quat}), 137.9 (C_{quat}), 141.0 (C_{quat}), 163.4 (C_{quat}), 164.8 (C_{quat}), 165.3 (C_{quat}). EI + MS (*m/z*): 376 (100) [M⁺], 273 (64) [C₁₆H₁₀F₃N⁺], 204 (47), 170 (24) [C₉H₅F₃⁺], 102 (33) [C₇H₄N⁺]. FT-IR: $\tilde{\nu}$ (cm⁻¹) = 631 (m), 650 (m), 681 (s), 737 (s), 752 (m), 826 (m), 841 (m), 1001 (m), 1016 (m), 1067 (s), 1109 (s), 1157 (m), 1321 (s), 1362 (m), 1497 (m), 1518 (m), 1530 (m), 1568 (m), 1589 (m), 3040 (w), 3065 (w). Anal. Calcd for C₂₃H₁₃F₃N₂ (376.4): C, 73.40; H, 4.02; N, 7.44. Found: C, 73.23; H, 3.45; N, 7.37.

4-(4-Chlorophenyl)-2,6-diphenylpyrimidine (8e). According to GP2 using 1-chloro-4-iodobenzene and benzoyl chloride, 147 mg (0.429 mmol, 43%) of **8e** was obtained as a light yellow solid. Purification was performed using the flash purification system, followed by recrystallization from *n*-hexane (25 mL). Mp: 162–164 °C (lit.³⁰ mp 160–161 °C). ¹H NMR (CDCl₃, 300 MHz): δ 7.50–7.61 (m, 8 H), 7.95 (s, 1 H), 8.20–8.31 (m, 4 H), 8.68–8.74 (m, 2 H). ¹³C NMR (CDCl₃, 75 MHz): δ 110.1 (CH), 127.4 (CH), 128.59 (CH), 128.60 (CH), 128.7 (CH), 129.1 (CH), 129.3 (CH), 130.9 (CH), 131.0 (CH), 136.0 (C_{quat}), 137.1 (C_{quat}), 137.5 (C_{quat}), 138.1 (C_{quat}), 163.6 (C_{quat}), 164.7 (C_{quat}), 165.0 (C_{quat}). EI + MS (*m/z*): 344 (30) [M⁺, ³⁷Cl], 342 (90) [M⁺, ³⁵Cl], 241 (9) [C₁₅H₁₀³⁷ClN⁺], 239 (26) [C₁₅H₁₀³⁵ClN⁺], 204 (100) [C₁₅H₁₀N⁺], 138 (10) [C₈H₅³⁷Cl⁺], 136 (28) [C₈H₅³⁵Cl⁺], 102 (35) [C₇H₄N⁺]. FT-IR: $\tilde{\nu}$ (cm⁻¹) = 658 (m), 687 (s), 750 (s), 775 (m), 820 (m), 1092 (m), 1360 (s), 1491 (m), 1526 (s), 1568 (s), 1589 (m), 3030 (w), 3055 (w), 3092 (w). Anal. Calcd for C₂₂H₁₅ClN₂ (342.8): C, 77.08; H, 4.41; N, 8.17. Found: C, 76.82; H, 4.22; N, 7.98.

4-(4-Bromophenyl)-6-(3-chlorophenyl)-2-phenylpyrimidine (8f). According to GP2 using 1-bromo-4-iodobenzene and 3-chlorobenzoyl chloride, 207 mg (0.491 mmol, 49%) of **8f** was obtained as a beige

solid. Purification was performed using the flash purification system, followed by recrystallization from *n*-hexane (23 mL). Mp 128–129 °C (lit.³¹ mp 130–132 °C). ¹H NMR (CDCl₃, 600 MHz): δ 7.47–7.56 (m, 5 H), 7.67–7.69 (m, 2 H), 7.89 (s, 1 H), 8.11–8.15 (m, 3 H), 8.246–8.254 (m, 1 H), 8.66–8.68 (m, 2 H). ¹³C NMR (CDCl₃, 150 MHz): δ 110.0 (CH), 125.5 (CH), 125.8 (C_{quat}), 127.5 (CH), 128.6 (CH), 128.7 (CH), 128.9 (CH), 130.3 (CH), 131.0 (CH), 131.1 (CH), 132.3 (CH), 135.3 (C_{quat}), 136.2 (C_{quat}), 137.8 (C_{quat}), 139.3 (C_{quat}), 163.6 (C_{quat}), 164.0 (C_{quat}), 164.8 (C_{quat}). EI + MS (*m/z*): 424 (7) [M⁺, ⁸¹Br, ³⁷Cl], 422 (26) [M⁺, ⁸¹Br, ³⁵Cl], 420 (21) [M⁺, ⁷⁹Br, ³⁵Cl], 362 (50) [C₁₇H₁₂⁸¹Br³⁷ClN₂⁺], 360 (100) [C₁₇H₁₂⁸¹Br³⁵ClN₂⁺], 358 (52) [C₁₇H₁₂⁷⁹Br³⁵ClN₂⁺], 284 (11) [C₁₅H₉⁸¹BrN⁺], 282 (13) [C₁₅H₉⁷⁹BrN⁺], 238 (22), 200 (53), 180 (18), 174 (13), 139 (17), 136 (12), 100 (21), 75 (10). FT-IR: $\tilde{\nu}$ (cm⁻¹) = 637 (m), 654 (m), 683 (s), 725 (s), 748 (s), 789 (m), 824 (m), 835 (m), 1074 (m), 1360 (s), 1477 (m), 1487 (m), 1526 (s), 1564 (s), 1587 (m), 3038 (w), 3063 (w). Anal. Calcd for C₂₂H₁₄BrClN₂ (421.7): C, 62.66; H, 3.35; N, 6.64. Found: C, 62.50; H, 3.10; N, 6.43.

■ ASSOCIATED CONTENT

Supporting Information

The Supporting Information is available free of charge on the ACS Publications website at DOI: 10.1021/acs.joc.6b01326.

NMR spectra of compounds **6** and **8**; absorption and emission spectra of pyrazoles **6a,i–p**; computational data and TD-DFT computed UV/vis spectra of pyrazoles **6a,i–p** (PDF)

■ AUTHOR INFORMATION

Corresponding Author

*E-mail: thomasjj.mueller@uni-duesseldorf.de.

Notes

The authors declare no competing financial interest.

[†]ISHC member.

■ ACKNOWLEDGMENTS

We cordially thank the Fonds der Chemischen Industrie and the Deutsche Forschungsgemeinschaft (Mu 1088/9-1) for financial support. We gratefully acknowledge Dr. Melanie Denißen for advice on the photophysical characterization of pyrazoles **6**.

■ DEDICATION

Dedicated to the memory of Prof. Dr. Rudolf Gompper (1926–1999).

■ REFERENCES

- (1) (a) Lanke, S. K.; Sekar, N. *Dyes Pigm.* **2016**, *127*, 116–127. (b) Lanke, S. K.; Sekar, N. *Dyes Pigm.* **2016**, *126*, 62–75. (c) Sarkar, A.; Chakravorti, S. *Chem. Phys. Lett.* **1995**, *235*, 195–201. (d) Vollmer, F.; Rettig, W.; Birckner, E. *J. Fluoresc.* **1994**, *4*, 65–69.
- (2) (a) Dorlars, A.; Schellhammer, C.-W.; Schroeder, J. *Angew. Chem., Int. Ed. Engl.* **1975**, *14*, 665–679. (b) Wang, X.; Li, W.; Zhang, X.-H.; Liu, D.-Z.; Zhou, X.-Q. *Dyes Pigm.* **2005**, *64*, 141–146.
- (3) Catalan, J.; Fabero, F.; Claramunt, R. M.; Santa Maria, M. D.; Foces-Foces, M. d. l. C.; Hernandez Cano, F.; Martinez-Ripoll, M.; Elguero, J.; Sastre, R. *J. Am. Chem. Soc.* **1992**, *114*, 5039–5048.
- (4) (a) Pandian, T. S.; Choi, Y.; Srinivasadesikan, V.; Lin, M.-C.; Kang, J. *New J. Chem.* **2015**, *39*, 650–658. (b) Ren, T.; Wang, J.; Li, G.; Li, Y. *J. Fluoresc.* **2014**, *24*, 1149–1157. (c) Yang, Z.; Zhang, K.; Gong, F.; Li, S.; Chen, J.; Ma, J. S.; Sobenina, L. N.; Mikhaleva, A. I.; Trofimov, B. A.; Yang, G. *J. Photochem. Photobiol., A* **2011**, *217*, 29–34.
- (5) (a) For a recent monograph, see: Müllen, K., Scherf, U., Eds.; *Organic Light-Emitting Diodes – Synthesis, Properties, and Applications*;

Wiley-VCH: Weinheim, 2006. (b) Chen, X.-L.; Yu, R.; Zhang, Q.-K.; Zhou, L.-J.; Wu, X.-Y.; Zhang, Q.; Lu, C.-Z. *Chem. Mater.* **2013**, *25*, 3910–3920. (c) Ma, C. Q.; Zhang, L. Q.; Zhou, J. H.; Wang, X. S.; Zhang, B. W.; Cao, Y.; Bugnon, P.; Schaer, M.; Nuesch, F.; Zhang, D. Q.; Qiu, Y. *J. Mater. Chem.* **2002**, *12*, 3481–3486.

(6) Xia, J.-B.; Li, F.-Y.; Yang, H.; Li, X.-H.; Huang, C.-H. *J. Mater. Sci.* **2007**, *42*, 6412–6416.

(7) (a) For the concept of diversity-oriented synthesis, see, e.g.: Burke, M. D.; Schreiber, S. L. *Angew. Chem., Int. Ed.* **2004**, *43*, 46–58.

(b) For diversity-oriented syntheses of functional π -systems, see: Müller, T. J. J.; D'Souza, D. M. *Pure Appl. Chem.* **2008**, *80*, 609–620.

(8) For a very recent review on MCR syntheses of functional π -systems, see: Levi, L.; Müller, T. J. J. *Chem. Soc. Rev.* **2016**, *45*, 2825–2846.

(9) (a) Denißen, M.; Nordmann, J.; Dziambor, J.; Mayer, B.; Frank, W.; Müller, T. J. J. *RSC Adv.* **2015**, *5*, 33838–33854. (b) Willy, B.; Müller, T. J. J. *Eur. J. Org. Chem.* **2008**, *2008*, 4157–4168.

(10) Lessing, T.; Müller, T. J. J. *Appl. Sci.* **2015**, *5*, 1803–1836.

(11) (a) Willy, B.; Müller, T. J. J. *Curr. Org. Chem.* **2009**, *13*, 1777–1790. (b) Chemler, S. R.; Fuller, P. H. *Chem. Soc. Rev.* **2007**, *36*, 1153–1160.

(12) Negishi, E.-i.; Kitora, M.; Xu, C. *J. Org. Chem.* **1997**, *62*, 8957–8960.

(13) Götzinger, A. C.; Müller, T. J. J. *Org. Biomol. Chem.* **2016**, *14*, 3498–3500.

(14) Willy, B.; Müller, T. J. J. *Org. Lett.* **2011**, *13*, 2082–2085.

(15) Karpov, A. S.; Müller, T. J. J. *Synthesis* **2003**, 2815–2826.

(16) Buck, C.; Gramlich, B.; Wagner, S. *J. Instrum.* **2015**, *10*, P09007.

(17) Grabowski, Z. R.; Rotkiewicz, K.; Rettig, W. *Chem. Rev.* **2003**, *103*, 3899–4032.

(18) Fery-Forgues, S.; Lavabre, D. *J. Chem. Educ.* **1999**, *76*, 1260–1264.

(19) Lakowicz, J. R. *Principles of Fluorescence Spectroscopy*, 3rd ed.; Springer: Berlin, 2006.

(20) Lippert, E. *Z. Elektrochem., Ber. Bunsenges. Phys. Chem.* **1957**, *61*, 962–975.

(21) (a) Lee, C.; Yang, W.; Parr, R. G. *Phys. Rev. B: Condens. Matter Mater. Phys.* **1988**, *37*, 785–789. (b) Becke, A. D. *J. Chem. Phys.* **1993**, *98*, 1372–1377. (c) Kim, K.; Jordan, K. D. *J. Phys. Chem.* **1994**, *98*, 10089–10094. (d) Stephens, P. J.; Devlin, F. J.; Chabalowski, C. F.; Frisch, M. J. *J. Phys. Chem.* **1994**, *98*, 11623–11627.

(22) Krishnan, R.; Binkley, J. S.; Seeger, R.; Pople, J. A. *J. Chem. Phys.* **1980**, *72*, 650–654.

(23) Scalmani, G.; Frisch, M. J. *J. Chem. Phys.* **2010**, *132*, 114110.

(24) Yanai, T.; Tew, D. P.; Handy, N. C. *Chem. Phys. Lett.* **2004**, *393*, 51–57.

(25) Kong, Y.; Tang, M.; Wang, Y. *Org. Lett.* **2014**, *16*, 576–579.

(26) Ren, Z.; Cao, W.; Chen, J.; Wang, Y.; Ding, W. *J. Heterocycl. Chem.* **2006**, *43*, 495–497.

(27) Nikpour, F.; Beigvand, M. *Monatsh. Chem.* **2008**, *139*, 821–824.

(28) Zhdanova, M. P.; Zvezdina, É. A.; Dorofeenko, G. N. *Chem. Heterocycl. Compd.* **1978**, *14*, 371–373.

(29) Forrester, A. R.; Gill, M.; Sadd, J. S.; Thomson, R. H. *J. Chem. Soc., Perkin Trans. 1* **1979**, *1*, 612–615.

(30) Adib, M.; Mahmoodi, N.; Mahdavi, M.; Bijanzadeh, H. R. *Tetrahedron Lett.* **2006**, *47*, 9365–9368.

(31) Vadagaonkar, K. S.; Kalmode, H. P.; Prakash, S.; Chaskar, A. C. *New J. Chem.* **2015**, *39*, 3639–3645.